Available online at www.sciencedirect.com
ScienceDirect
Journal of Crystal Growth 299 (2007) 59–62
JOURNAL OF CRYSTAL GROWTH
www.elsevier.com/locate/jcrysgro

Comparative study of n-type AlGaN grown on sapphire by using a superlattice layer and a low-temperature AlN interlayer

Y.A. Xi[a,b], K.X. Chen[a,b], F. Mont[a,c], J.K. Kim[a,c], E.F. Schubert[a,b,c,*], W. Liu[d], X. Li[d], J.A. Smart[d]

[a]*Future Chips Constellation, Rensselaer Polytechnic Institute, 110, 8th Street, Troy, NY 12180, USA*
[b]*Department of Physics, Applied Physics, and Astronomy, Rensselaer Polytechnic Institute, 110, 8th Street, Troy, NY 12180, USA*
[c]*Department of Electrical, Computer, and Systems Engineering, Rensselaer Polytechnic Institute, 110, 8th Street, Troy, NY 12180, USA*
[d]*Crystal IS, Inc., Green Island, NY 12183, USA*

Received 13 June 2006; received in revised form 20 October 2006; accepted 24 October 2006
Communicated by R.M. Biefeld
Available online 3 January 2007

Abstract

Si-doped $Al_{0.3}Ga_{0.7}N$ grown on (0 0 0 1)-oriented sapphire is optimized by using a superlattice (SL) layer. Atomic force microscopy (AFM), high-resolution X-ray diffraction (HRXRD), secondary ion mass spectrometry (SIMS), and Hall effect measurements show that n-type $Al_{0.3}Ga_{0.7}N$ grown on a SL layer gives high-quality crystalline and electrical properties. A 1.8-μm-thick crack-free n-type $Al_{0.3}Ga_{0.7}N$ layer is demonstrated with a doping concentration of $3 \times 10^{18}\,cm^{-3}$, an excellent mobility of $80\,cm^2/(V\,s)$, and an RMS roughness of 0.40 nm. Using the SL layer also results in the absence of hexagonal hillocks on the AlGaN surface, which are indicative of a high defect density. The study of an identical n-type $Al_{0.3}Ga_{0.7}N$ layer grown on a low-temperature AlN interlayer shows a lower carrier concentration, mobility, and crystalline quality.

PACS: 81.15.Gh; 81.05.Ea; 78.55.Cr; 73.61.Ey

Keywords: A3. Metalorganic vapor phase epitaxy; B1. AlGaN; B1. Nitride; B3. Light emitting diode

AlGaN-based ultra-violet (UV) light-emitting diodes (LEDs) are expected to greatly impact a number of applications including fluorescence-based biological agent detection, water purification, sterilization, decontamination, non-line-of-sight (NLOS) communications, and thin-film curing [1]. Si-doped $Al_xGa_{1-x}N$ is a key material in UV LED structures since it is not only the n-type contact layer that supplies electrons to the active region, but also the buffer layer and therefore must be of high crystalline quality. However, strain between the AlN and the AlGaN, which is due to the different lattice constants, induces cracks and dislocations. The strain depends on the crystal orientation [2], the thickness, and the chemical composition of the epitaxial layers [3]. Strain engineering [4] can be accomplished by superlattice (SL) layers [5], low-temperature (LT) AlN interlayers [6], homoepitaxial substrates [7,8], and non-polar substrates [9–12]. Among these approaches, AlGaN/AlGaN SLs and LT AlN interlayers are frequently used on (0 0 0 1)-oriented sapphire substrates. An additional function of SL layers is to work as a dislocation filter [5].

In this paper, two AlGaN/AlN structures, grown by metalorganic vapor phase epitaxy (MOVPE), are studied, namely an AlGaN(AlN)/AlGaN SL, and a LT AlN interlayer. It is found that by using a SL layer, the critical thickness of a Si-doped $Al_{0.3}Ga_{0.7}N$ layer can be greater than 2.0 μm. Atomic force microscopy (AFM),

*Corresponding author. Department of Electrical, Computer, and Systems Engineering, Rensselaer Polytechnic Institute, 110, 8th Street, Troy, NY 12180, USA. Tel.: +518 276 8775; fax: 518 276 8042.
E-mail address: efschubert@rpi.edu (E.F. Schubert).

0022-0248/$ - see front matter © 2006 Elsevier B.V. All rights reserved.
doi:10.1016/j.jcrysgro.2006.10.253

high-resolution X-ray diffraction (HRXRD), and Hall effect measurements show that samples with a SL layer give a much better crystalline quality and electric properties than samples using LT AlN interlayers.

In order to investigate the improvement of n-type $Al_{0.3}Ga_{0.7}N$ layers by using SL layers and LT interlayers, two types of structures are demonstrated and for each type, several samples have been grown and characterized. The results are very similar and thus reproducible. Here, we present a typical result from each type. All samples are grown using a 5.0 cm single-wafer horizontal-flow reactor with radio-frequency induction heating. The structures of the two samples are shown in Fig. 1. For both types of samples, we first grow a 300-nm-thick AlN buffer layer at a reactor temperature of 1205 °C and a pressure of 25 mbar on the top of an AlN nucleation layer grown at 812 °C and 50 mbar. The V/III ratio for both, the high-temperature (HT) AlN buffer layer and AlN nucleation layer is 5370. In sample type (a), a 10 period 15-nm AlN/15-nm $Al_{0.7}Ga_{0.3}N$ SL followed by a 10 period 15-nm $Al_{0.7}Ga_{0.3}N$/15-nm $Al_{0.54}Ga_{0.46}N$ is grown on the HT AlN buffer layer. In sample type (b), a LT AlN interlayer is grown at 812 °C and 50 mbar on top of the HT AlN buffer layer. The two types of samples are finished with an identical 1.8 μm thick Si-doped n-type $Al_{0.3}Ga_{0.7}N$ layer with a doping level of $4 \times 10^{18}\,cm^{-3}$, measured by using secondary ion mass spectrometry (SIMS), accomplished by a silane flow of 4.9×10^{-9} mol/min.

After growth, no cracks are found on sample (a) and no hexagonal hillocks are observed by optical microscopy, as shown in Fig. 2(a). But sample (b), with the LT AlN interlayer, is found to be cracked at the perimeter of the wafer and many hexagonal hillocks are found on the surface, as shown in Fig. 2(b), which were identified as regions with a high defect density [13].

In order to explore the crystalline quality and electric properties, the AFM, HRXRD, and Hall effect measurements are performed on the two types of samples. Fig. 3 shows the AFM images of the two samples. The RMS roughness and dislocation density are summarized in Table 1, which also includes HRXRD and Hall results. The dislocation density is also evaluated from the AFM images, which is obtained by averaging the pit densities on different spots of the sample and with different image sizes (1 μm × 1 μm size and 2 μm × 2 μm size). Sample (a) shows an RMS roughness of 0.40 nm. Sample (b) has a roughness of 0.50 nm. Meanwhile, inspection of Fig. 3 reveals that the SLs decrease the dislocation density by working as a defect filter. The dislocation density measured from the AFM images decreases from $9 \times 10^{9}\,cm^{-2}$ for sample (b) to $5 \times 10^{9}\,cm^{-2}$ for sample (a). The absence of hexagonal hillocks on sample (a) indicates that sample (a) is of high crystalline quality.

Hall effect measurements at room temperature reveal that the mobility and carrier concentration of sample (a) are higher than that of sample (b). Sample (a) has a carrier concentration of $3 \times 10^{18}\,cm^{-3}$. Generally, there are two types of donors in n-type AlGaN: one type is an effective mass-like state located ~30–60 meV below the conduction band; the other type, which has a defect-related metastable character, is localized deeper in the band gap of AlGaN [14]. Our results suggest that at a doping level of

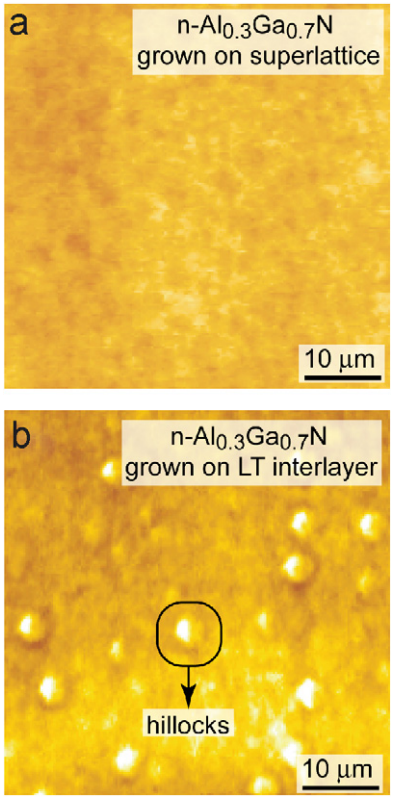

Fig. 2. Optical micrographs of sample (a) grown on AlGaN(AlN)/AlGaN SL, showing no hillocks and sample (b) grown on an LT AlN interlayer, showing several hillocks.

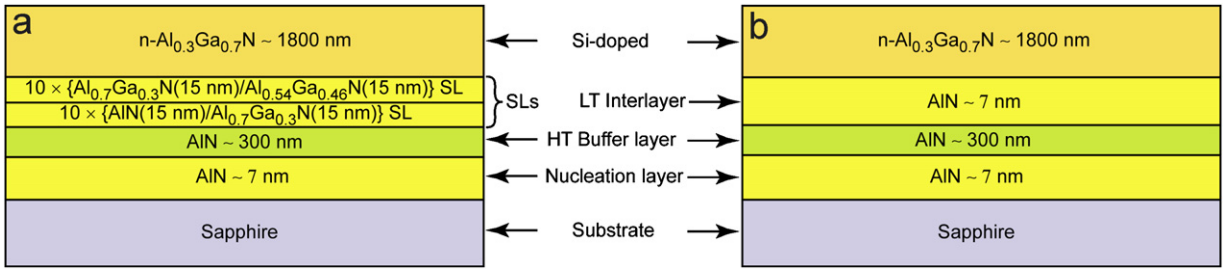

Fig. 1. Schematic of two different structures that use an AlGaN(AlN)/AlGaN SL and a LT AlN interlayer.

$4 \times 10^{18}\,cm^{-3}$, the concentration of the defect-related metastable states may be reduced by applying a SL, which could result in the possibility that Si atoms act as effective mass states so that a higher carrier density at room temperature becomes possible. By inserting two sets of SLs, the defect-filter function of SLs in sample (a) further reduces the dislocation density and increases the mobility.

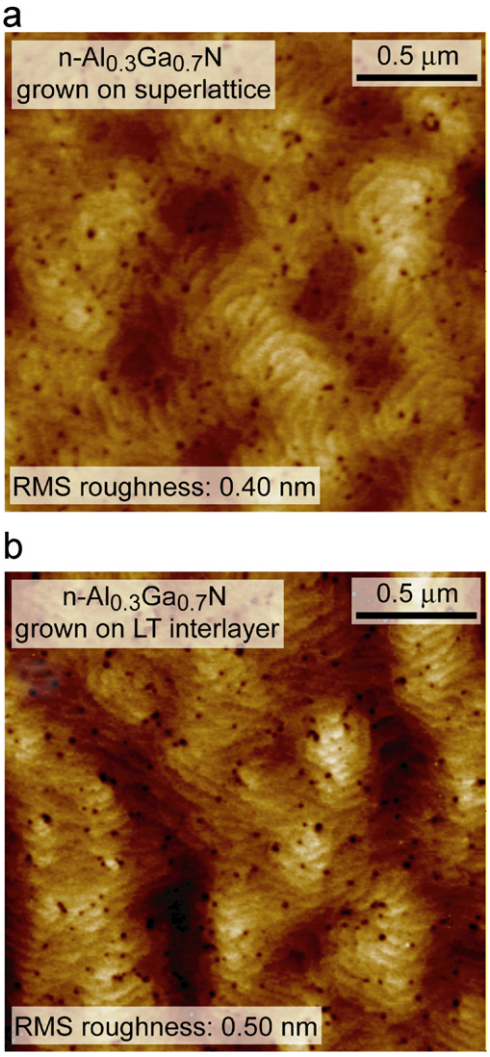

Fig. 3. AFM images of sample (a) grown on AlGaN(AlN)/AlGaN SL, showing lower dislocation density and sample (b) grown on an LT AlN interlayer, showing higher dislocation density.

The X-ray rocking curve scan of the (0 0 2) peak is measured and shown in Fig. 4. It is found that sample (a) has a narrower FWHM than sample (b), which indicates that the SL further improves the crystalline quality of AlGaN. The (1 0 1) peak is also measured and the FWHM of sample (a) and sample (b) is 37.6 arcmin and 47.8 arcmin, respectively. From the X-ray line width, the screw dislocation density and the edge dislocation density are evaluated [15] and it is found that the screw dislocation density of samples (a) and (b) is 2.3×10^9 and $2.5 \times 10^9\,cm^{-2}$, respectively, and the edge dislocation density of samples (a) and (b) is 3.4×10^{10} and 4.3×10^{10} cm^{-2}, respectively. The screw dislocation density evaluated by using X-ray line width is in good agreement with the AFM-measured dislocation density. This is consistent with the suggestion that the pits found on the AFM images are due to the intersection of screw component dislocations with the surface [16]. The screw and edge dislocation results reveal that SLs reduce both the screw and edge dislocations. Furthermore, a strong reduction of the edge dislocation density is found by using SLs. In the present study, it is also found that the critical thickness of the n-type $Al_{0.3}Ga_{0.7}N$ is greater than 2.0 μm by using AlGaN/AlGaN SL method.

In conclusion, two MOVPE-grown AlGaN/AlN structures are studied that use an AlGaN(AlN)/AlGaN SL and a LT AlN interlayer. It is found that by using the SL, the critical thickness of Si-doped $Al_{0.3}Ga_{0.7}N$ layer is greater than 2 μm. The AFM, HRXRD, and Hall effect

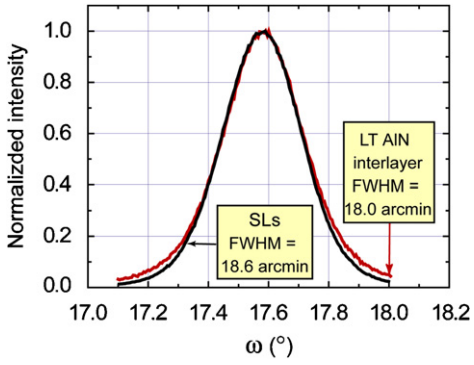

Fig. 4. (0 0 2) rocking curve of sample (a) grown on AlGaN(AlN)/AlGaN SL showing narrower X-ray linewidth and sample (b) grown on an LT AlN interlayer, showing a broader X-ray linewidth.

Table 1
Electron mobility, carrier concentration, surface roughness, dislocation densities, and X-ray linewidth of sample (a) grown on AlGaN(AlN)/AlGaN SL and sample (b) grown on an LT AlN interlayer

$Al_{0.3}Ga_{0.7}N$ on sapphire	n (cm^{-3})	μ ($cm^2/(V\,s)$)	Surface RMS roughness (nm)	AFM dislocation density (cm^{-3})	XRD			
					edge dislocation density (cm^{-2})	Screw dislocation density (cm^{-2})	FWHM of (0 0 2) (arcmin)	FWHM of (1 0 1) (arcmin)
SL	3.0×10^{18}	80	0.40	5.0×10^9	3.4×10^{10}	2.3×10^9	18	37.4
LT interlayer	2.0×10^{18}	40	0.50	9.0×10^9	4.3×10^{10}	2.5×10^9	18.6	41.8

measurements also show that the sample with the SL gives the best results in terms of crystalline quality and electric properties. 1.8-μm-thick Si-doped $Al_{0.3}Ga_{0.7}N$ layer is obtained by using the SL. An XRD-deduced edge dislocation density and screw dislocation density of 3.4×10^{10}, $2.3 \times 10^{9}\,cm^{-2}$, respectively, carrier concentration of $3 \times 10^{18}\,cm^{-3}$, mobility of $80\,cm^2/(V\,s)$, and an RMS roughness of 0.40 nm are obtained on the AlGaN layer. Using the SL also results in the absence of hexagonal hillocks that are indicative of high defect density.

Support through the Crystal IS, Department of Energy, ARO, the Samsung Advanced Institute of Technology, Sandia National Laboratories, NSF, and New York state is gratefully acknowledged. The authors would like to acknowledge useful discussions with Dr. Thomas Gessmann and Mr. Jan-Yves Clames from Aixtron.

References

[1] A.A. Allerman, M.H. Crawford, A.J. Fischer, K.H.A. Bogart, S.R. Lee, D.M. Follstaedt, P.P. Provencio, D.D. Koleske, J. Crystal Growth 272 (2004) 227.
[2] A. Bykhovski, B. Gelmont, M.S. Shur, Appl. Phys. Lett. 2243 (1993) 63.
[3] M.A. Khan, J.W. Yang, G. Simin, H. zur Loye, R. Bicknell-Tassius, R. Gaska, M.S. Shur, G. Tamulaitis, A. Žukauskas, Phys. Stat. Sol. A 227 (1999) 176.
[4] Y. S. Park, M. S. Shur, W. Tang, Frontiers in Electronics: Future Chips, Singapore, 2003, p. 195
[5] D. Bykhovski, B.L. Gelmont, M.S. Shur, Proc. Int. Semicond. Dev. Res. Symp. 541 (1995) 2.
[6] H. Amano, M. Iwaya, T. Kashima, M. Katsuragawa, I. Akasaki, J. Han, S. Hearne, J. Floro, E. Chason, J. Figiel, Jpn. J. Appl. Phys. L 1540 (1998) 37.
[7] X. Hu, J. Deng, N. Pala, R. Gaska, M.S. Shur, C.Q. Chen, J. Yang, S. Simin, M.A. Khan, C. Rojo, L.J. Schowalter, Appl. Phys. Lett. 1299 (2003) 82.
[8] R. Gaska, C. Chen, J. Yang, E. Kuokstis, M.A. Khan, G. Tamulaitis, I. Yilmaz, M.S. Shur, J.C. Rojo, L.J. Schowalter, Appl. Phys. Lett. 4658 (2002) 81.
[9] S. Ghosh, P. Waltereit, O. Brandt, H.T. Grahn, K.H. Ploog, Phys. Rev. B 075202 (2002) 65.
[10] P. Waltereit, O. Brandt, M. Ramsteiner, R. Uecker, P. Reiche, K.H. Ploog, J. Crystal Growth 143 (2000) 218.
[11] W.H. Sun, J.W. Yang, C.Q. Chen, J.P. Zhang, M.E. Gaevski, E. Kuokstis, V. Adivarahan, H.M. Wang, Z. Gong, M. Su, M.A. Khan, Appl. Phys. Lett. 2599 (2003) 83.
[12] W.H. Sun, E. Kuokstis, M. Gaevski, J.P. Zhang, C.Q. Chen, H.M. Wang, J.W. Yang, G. Simin, M.A. Khan, R. Gaska, M.S. Shur, Phys. Stat. Sol. A 48 (2003) 200.
[13] Q. Liu a, H. Lakner, A. Meinert, F. Scholz, A. Sohmer, E. Kubalek, Mater. Sci. Eng. B 245 (1997) 50.
[14] C. Skierbiszewski, T. Suski, M. Leszcynski, M. Shin, M. Skowronski, M.D. Bremser, R.F. Davis, Appl. Phys. Lett. 3833 (1999) 74.
[15] S.R. Lee, A.M. West, A.A. Allerman, K.E. Waldrip, D.M. Follstaedt, P.P. Provencio, D.D. Koleske, Appl. Phys. Lett. 86 (2005) 241904.
[16] B. Heying, E.J. Tarsa, C.R. Elsass, P. Fini, S.P. Denbaars, J.S. Speck, J. Appl. Phys. 85 (1999) 6470.